4. Spain, J., 1997. "Evaluation of CFRP/Concrete Bond Under Shear and Tension," Master's Thesis, University of South Florida, Tampa, FL.

5. Bedford, A. and Wallace L. Fowler, 1995. *"Statics–Engineering Mechanics"* Addison-Wesley Publishing, Reading, MA.

TABLE 1—SUMMARY OF TEST RESULTS.

Label	Number Of Specimens	Shear Stress from Tr/J		Percent Debond	Tension Stress from P/A		Percent Debond
		ksi	MPa		ksi	MPa	
N3U	4	1.86	12.8	40	0.49	3.4	7.5
N3B	4	1.52	10.5	0.0	0.49	3.4	6.7
M3U	4	1.86	12.8	6.3	0.52	3.6	16.5
W3U	4	1.65	11.4	20.0	0.57	3.9	7.5
M5U	4	1.32	9.1	1.3	0.38	2.6	0.0
W5U	6	1.47	10.1	3.0	0.55	3.8	0.0

Fig. 1—Tension/shear setup.

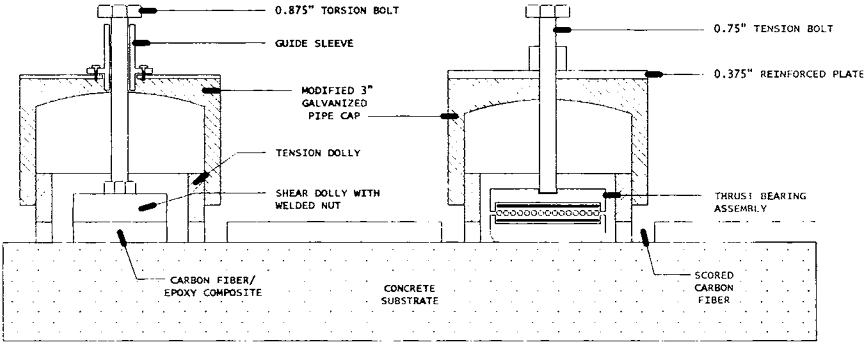

Fig. 2—Schematic drawing of shear (left) and tension (right) test apparatus.

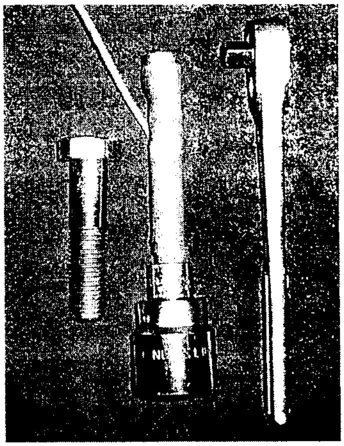

Fig. 3—Instrumented wrench.

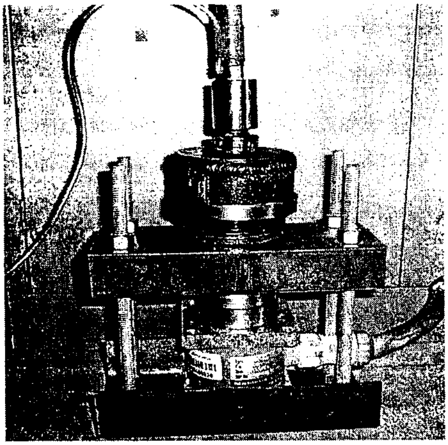

Fig. 4—Tension device calibration.

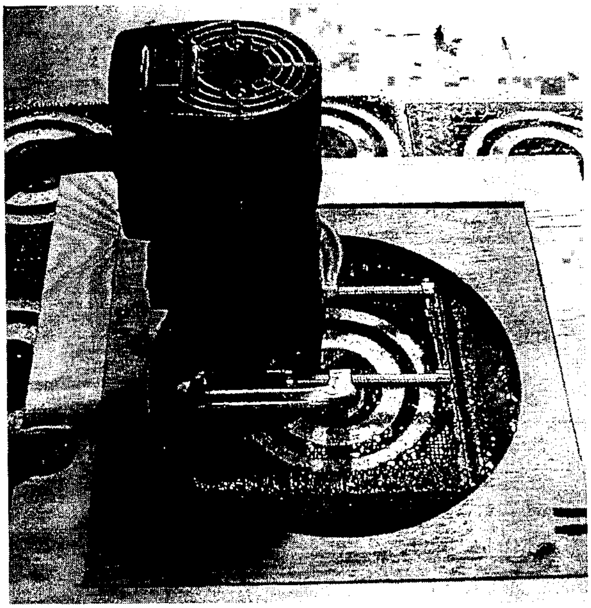

Fig. 5—CFRP scoring.

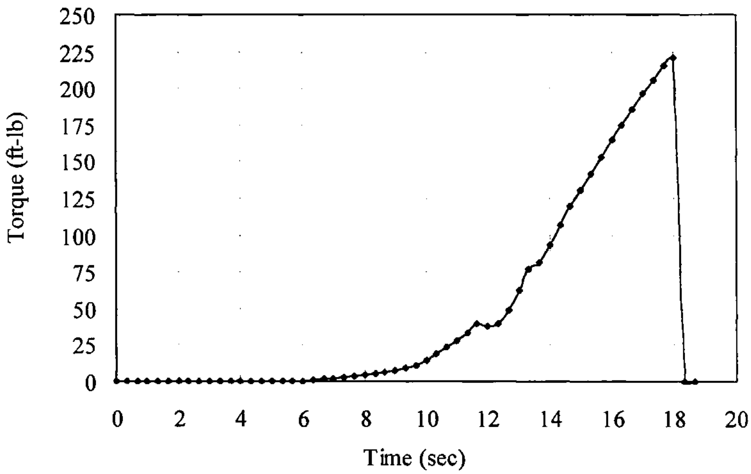

Fig. 6—Torque versus time during shear test.

SP 188-36

Bond of Glass Fiber Reinforced Plastic Reinforcing Bar for Consideration in Bridge Decks

by C. K. Shield, C. W. French, and J. P. Hanus

Synopsis:

The use of non-metallic bridge deck reinforcement is of interest in regions where corrosion is a problem. A number of manufacturers have developed GFRP rebar for this application. Because the production of the material is relatively new, there is a great deal of variability among the products from different manufacturers. In addition, as the manufacturers continue to develop their own product, variations in GFRP from single manufacturers have been observed.

The objective of this study was to investigate the bond between GFRP reinforcement and concrete using inverted half-beam specimen. The inverted half-beam specimen were designed to simulate the conditions likely to be found in a bridge deck (no transverse reinforcement and small concrete cover). Products from two different manufacturers were chosen for the study because of the widely varying characteristics of the product. One manufacturer produced reinforcement with surface deformations created by a helical wrap of glass fibers around the GFRP bar; the other manufacturer developed a ceramic coating that emulated the surface texture of a deformed steel bar.

The two different bar types exhibited different bond behaviors. The bond for the bars with the ceramic deformations relied most heavily on mechanical interlock, as was evident from cracking patterns. The bond for the bars with the helical wrap deformations relied most heavily on friction. Both bar types demonstrated large variability for the bond specimen that failed in bar fracture, with some bar failure loads more than two standard deviations below the average bar tensile strength.

Keywords: bond; glass fiber reinforced plastic; reinforcing bar; tests

Carol K. Shield is an Associate Professor in the Department of Civil Engineering at the University of Minnesota and an Associate Member of ACI 440.

Catherine W. French is a Professor in the Department of Civil Engineering at the University of Minnesota and a member of ACI Committees 318, 408, 423, and 445.

Joseph P. Hanus is an instructor at West Point Academy.

INTRODUCTION

For more than 100 years, steel bars have performed well as a reinforcing medium in concrete structures until extensive application of de-icing salts to bridges and highways began in the late 1960's [1]. Since then corrosion has become a serious concern. Several methods have been used to reduce or delay the corrosion of steel reinforcement such as improving the impermeability of concrete and the use of epoxy-coated steel rebars. However, premature corrosion of epoxy-coated rebars has been found in bridges [2], which indicates a shortcoming of this technique.

As a result, in the last 15 years there has been an increase in the use of alternative reinforcing materials for concrete in harsh environments. Recent advancements in the field of plastics and fiber composites have resulted in the development of fiber reinforced plastic (FRP) rebar that surpass the strength and fatigue properties of steel. Although many researchers have studied development length of bond between glass fiber reinforced plastic (GFRP) and concrete [2-9], many questions still remain about differing bond mechanisms due to different bar types, as well as the inherent variability of GFRP reinforcing bars. Also, very few researchers have studied the development length of GFRP reinforcement with small concrete cover and no transverse reinforcement, which are likely to be the conditions found in bridge decks reinforced with GFRP rebar.

TEST PROGRAM

To investigate these issues, a total of 72 bond specimen were cast in 36 inverted half-beam specimen. The specimen were poured in two series, both using the same specified concrete. Bars having two distinctly different deformation systems were chosen for testing. Variables in the study included bar embedment length and concrete cover ($2d_b$ and $3d_b$). At least six repeats of each test were performed.

The inverted half-beam specimen were 12 in. wide, 18 in. deep and 48 in. long (Fig.1). Each beam had two test bars. The specimen were cast on their sides to eliminate top bar effects, with the test bars extending out opposite end faces, to facilitate the two separate tests to be carried out with each beam. Embedment lengths were controlled by shielding portions of the rebar with PVC pipe. Supplementary longitudinal reinforcement (No. 4 GRFP rebar) was added to prevent flexural failure in the unbonded regions of the test beams. The addition of this reinforcement was not intended to affect the bond behavior. No transverse reinforcement was used. It was not required for shear strength and its absence combined with a shallow concrete cover promoted a splitting bond failure (anticipated failure mode in bridge decks).

The specimen concrete was Type 3Y33, a typical Mn/DOT (Minnesota Department of Transportation) deck mix, with 6% air entrainment and a target strength of 4300 psi at 28 days (measured 28 day strengths were 6450 and 6340 psi for the two series).

The two bars selected for testing were No. 5 bars from Marshall Industries Composites, Inc. (M1), and No. 6 bars from Hughes Brothers/Corrosion Proof Products (M2). The M1 GFRP bars were constructed of 70% (weight) E-glass fibers in a 10% recycled polyester resin material and had a bar deformation system similar in appearance to that of steel rebar, consisting of a ceramic coating with a rib face angle greater than 40 degrees. The deformations were formed from 3.5% ceramic fibers embedded in a 15% urethane modified vinyl ester matrix with a 1.5% corrosion inhibitor. The individual deformations (spaced at approximately 3/8 in.) were formed from a special molding process that was repeated along the bar at approximately 9 in. lengths. At the mold joints, the pattern for the bar deformation system was interrupted and some bars appeared to be "missing" deformations at these points due to the manufacturing process.

The second GFRP rebar tested was more typical of bars currently available. The M2 bars were constructed of 76% (weight) E-glass Owens Corning Type 30-366-133 fibers in a 24% blended vinylester resin matrix. The rebar had a deformation system formed from helically wrapped glass fibers with a pitch of approximately 1 in. This wrapped fiber system impressed into the bar core causing the bar to bulge between the wraps, creating a deformation. The resulting rib face angles were less than 30 degrees. The manufacturer coated the bars with sand after the deformation system was formed to provide additional frictional resistance.

Although the exact distribution of bond stress is complicated, the test embedment lengths were determined assuming a uniform bond stress distribution. This results in an assumed linear relationship between embedment length and bond strength as given by

$$l_{em} = K_1 \frac{f_t A_b}{\sqrt{f'_c}} \tag{1}$$

where l_{em} is the embedment length; K_1 is an empirical constant to account for factors such as confinement, surface condition, and bar properties; f'_c is the concrete compressive strength (assumed as 4300 psi); f_t is the target bond strength; and A_b is the reinforcement bar area (measured as 0.302 in^2 for M1 and 0.471 in^2 for M2 using the volume displacement method).

Initial values for K_1 (0.059 for M1 and 0.057 for M2) were obtained empirically by averaging the results of pilot tests. The embedment lengths were selected to achieve target bond strengths between 55 and 100% of the bar tensile strengths, f_u. In other words, these tests were designed to approach the development length. The tensile strengths of the bars were determined in accordance with ASTM D3916-94. To compare the effect of the $3d_b$ cover to $2d_b$ cover, two series of specimen were cast with similar embedment lengths. In addition, for each manufacturer, a set of bars was embedded the full length of the specimen with a $2d_b$ cover to ensure that full bar development was possible with a shallow cover. Based on these considerations, and the above mentioned variables, the embedment lengths for the M1 bars were calculated as 12.5, 15.0 and 47.0 in. for tests with $2d_b$ cover and 10.0, 12.5 and 15.0 in. for tests with $3d_b$ cover; and the embedment lengths for the M2 bars were calculated as 15.0, 20.0, 25.0, 47.0 in. for tests with $2d_b$ cover and 15.0 and 20.0 in. for tests with $3d_b$ cover.

The bond tests were performed when the specimen were between 38 and 149 days old, with three replicate tests conducted relatively early in the specimen life and the remaining three replicates tested later in the specimen life to even out changes in concrete strength over time. The specimen were loaded at a rate of 0.05 in/min until failure, as specified in ASTM C234. More details on the experimental setup can be found in Reference [10].

EXPERIMENTAL RESULTS

Bond and tensile test results are presented in Table 1. For each bond test series the table contains the following information for tests which failed in concrete splitting: concrete cover; embedment length; target bond strength as a percentage of the bar strength; the number of tests, average ultimate load, coefficient of variation (COV), and measured bond strength as a function of the bar strength. For tests that exhibited bar failures, the table lists the number and type of bar failures and average ultimate load. Average tensile strengths and COVs are reported in the table at the bottom of each section for bond tests that resulted in bar failures, "in air" tensile tests, and from the manufacturer's literature.

Six failure types were observed during bond testing: 1) Concrete splitting failures; 2) Bar failures inside the embedment that resulted in the bar breaking into separate strands resembling "spaghetti", identified by "SI" (Fig. 2); 3) Bar "spaghetti" failures outside the embedment ("SO"); 4) Bar "spaghetti" failures both inside and outside the embedment ("SB"); 5) Bar tensile failures with a complete perpendicular "fracture" of the bar ("F"), this failure was observed to occur in two M1 GFRP rebar tests at mold joints as shown in Fig. 3; and 6) Bar failures within the grip system ("G").

Variability

The average tensile strength of the M1 bars, as determined from ten tension tests (ASTM D3916-94), was 19.2 kips with a COV of 8.9%. The strength was more than 34% below the manufacturer's reported capacity of 29.4 kips. In addition, the measured variation was much larger than that indicated by the manufacturer. The tensile capacity of the M2 bars was determined from three tension tests as 43.5 kips (COV of 3.7%) which was equal to the manufacturer's reported strength; a COV was not supplied by the manufacturer.

Bar tensile fractures were observed in twenty-five M1 bond tests and eight M2 bond tests, as shown in Table 1. Averages and COVs for these tests are given at the bottom of the M1 and M2 sections of the table. For the M1 rebar, the average ultimate bar failure load for the twenty-five bar failures was 17.5 kips with a COV of 16.6%. This average was less than the average tensile test ultimate load of 19.2 kips and the manufacturer reported capacity of 29.4 kips. However, two of the bond test specimen bars exhibited bar failures at a mold joint (Fig. 3), yielding a significantly lower ultimate strength for these bars. If these bars are removed from consideration, then the average failure load of the remaining bar fractures was 18.0 kips (COV of 13.3%). This average was approximately 6% less than the "in air" tensile test average. This decrease in strength can be attributed to the small bending stresses imposed on the bar in the bond test. The average bending stress as measured by LVDTs attached to the bar would have lead to a decrease in tensile capacity of 1.8 ±0.6 kips for the specimen which failed in bar fracture.

All but one of the eight M2 rebar that exhibited bar failures failed in the grip. Even though the bars that failed in the grip did not reach their true ultimate load, the average ultimate load for all of the M2 bar fractures was 39.5 kips, which was only slightly below the tensile test average and manufacturer's reported tensile strength of 43.5 kips. The difference between these strengths was likely due to the induced bending stress in the bond test, as well as the decrease in strength associated with failures in the grip. The average measured bending stress indicated a 3.4 ± 1.2 kip reduction in tensile capacity. The one M2 bar that fractured in tension outside of the grip only reached a strength of 35.5 kips. This early failure of a fully embedded bar indicated that these bars can fail at less than 82% of the manufacturer's reported strength.

There were fourteen M1 bond tests and twenty-five M2 bond tests that exhibited concrete splitting failures as shown in Table 1. The coefficient of variation for bond strength for these tests ranged from 5.2 to 6.8 % for the M1 bars, and 3.2 to 13.1 % for the M2 bars. The largest COV for the M1 bars (6.8 %)

was observed for the series with $3d_b$ cover and 12.5 in embedment length (shortest embedment length). For the M1 bars, the variation in ultimate loads for the bond tests that failed in concrete splitting was most likely related to the rebar quality, as evinced by the lower COVs for the splitting failures than for the "in air" tension tests, with the highest COV for the shortest embedment length. Conversely, the variation for the M2 tests was more likely related to concrete variation and the variability in reproducing the testing procedures and setup for each test, evinced by an increase in COV over the "in air" tension tests and a general trend of increasing COVs with increasing embedment lengths. The largest COV for the M2 bars (13.1%) was observed in the series with $2d_b$ cover and a 25 in. embedment length. This larger COV may have been caused by the longer embedment length which allowed for a greater occurrence of concrete variation that could have influenced the variation in ultimate loads.

The large variability in all these tests indicates a potential problem when using GFRP rebar. Design strengths for these bars should be taken below the tensile test average minus two standard deviations, as both bar types exhibited bar failures below this value.

Development Length

The relationship between embedment length and ultimate load is plotted in Fig.4a and Fig.4b for the M1 and M2 bars, respectively. Each test that failed in concrete splitting is shown with a symbol corresponding to its associated cover. The tests that exhibited bar failures are shown without reference to cover. The average values for each embedment length are connected by lines for $2d_b$ (dash) and $3d_b$ (solid) cover. The average tensile test ultimate load of 19.2 kips for M1 and 43.5 kips for M2 are shown with horizontal dash-dot lines. In addition, the manufacturers reported strength (29.4 kips) is shown for M1 which was 53% higher than that measured in the University of Minnesota Laboratory. The manufacturers reported strength for the M2 bars was as tested, 43.5 kips. The dash-dot-dot lines represent the average tensile test value +/- two standard deviations. All the failure loads for the "in air" tensile tests were between these values.

As shown in Fig 4a, for M1, the majority of the ultimate loads for the bond tests were within +/- two standard deviations of the tensile test average failure load, with little increase in average failure load with increase in embedment length due to the large variability in bar strength. It appears that the development length for these bars is approximately 15.0 in., based on the observation that eleven of the twelve tests at this embedment length exhibited bar failure, while eleven of the fifteen tests at the next shorter embedment length (12.5 in.) exhibited splitting failures. However, even with a 15 in. or longer embedment length, several of these bars failed below two standard deviations of the tensile test average.

For the M2 bars, the majority of the tests fell below the two standard deviation line, failing in concrete splitting, as shown in Fig. 4b. It appears that the tested M2 embedment lengths only approached the development length. No tested embedment length (except the fully embedded bars) resulted in a majority of the tests exhibiting bar failures. However, a linear regression through the concrete splitting failures provides a minimum estimate of the development length for comparison. The linear regression through the concrete splitting failures intercepted the average bar tensile strength (43.5 kips) at a 31.5 in. embedment length. At the 47 in. embedment length, all the specimen exhibited bar failure (although only one bar reached the average tensile capacity), thus the development length for the M2 bars is between 31.5 and 47 in.

The effect of changing concrete cover from $2d_b$ to $3d_b$ can be seen to be minimal by examining Fig. 4. For the M1 bars, there were too few splitting failures to see a definite trend. The lack of effect of concrete cover for the splitting failures of the M2 specimen is not well understood. More tests need to be performed in order to evaluate the importance of concrete cover in the absence of transverse reinforcement.

Using these embedment lengths, the empirical constant K_1 of Eqn. (1) was determined as 0.063 for M1 and between 0.058 and 0.086 for M2. However, the use of these values of K_1 for different bar sizes, bar strengths and different concrete strengths has not been verified.

Bond Behavior

The most significant difference between the two GFRP rebar types was the general bond mechanism as observed in the analysis of the bond behavior. It is hypothesized that the M1 rebar relied primarily on mechanical interlock without significant adhesion or frictional resistance to develop bond along incremental portions of the embedment length. Comparatively, it is hypothesized that the M2 rebar relied primarily on friction, enhanced with adhesion, for bond resistance developed along the majority of the embedment length. It is believed that the M2 rebar did not develop any significant mechanical interlock. These hypotheses are based on analysis of the rebar surface condition, deformation geometry, crack patterns and forensic investigations as discussed below.

The rebar surface condition established the initial bond phase for each GFRP rebar type. The M1 rebar had a smooth ceramic outer coating and the M2 rebar had a rough sand coated surface. The smooth nature of the M1 rebar probably resulted in difficulty developing friction. The M1 rebar left visible impressions in the concrete. Although there did not appear to be concrete crushing around the M1 deformations, there was evidence of bearing on the M1 ceramic deformations, as an average of 37% of the deformations were sheared off. Comparatively, the M2